

Core Binding Factor Beta (*Cbfb*) Controls the Balance of Chondrocyte Proliferation and Differentiation by Upregulating Indian hedgehog (*Ihh*) Expression and Inhibiting Parathyroid Hormone-Related Protein Receptor (PPR) Expression in Postnatal Cartilage and Bone Formation

Fei Tian,^{1,2*} Mengrui Wu,^{2,3*} Lianfu Deng,¹ Guochun Zhu,² Junqing Ma,² Bo Gao,² Lin Wang,⁴ Yi-Ping Li,^{2#} and Wei Chen^{2#}

¹Shanghai Institute of Traumatology and Orthopedics, Ruijin Hospital, Jiao Tong University School of Medicine, Shanghai, People's Republic of China

²Department of Pathology, University of Alabama at Birmingham, AL, USA

³Institute of Genetics, Life Science College, Zhejiang University, Zhejiang, People's Republic of China

⁴Institute of Stomatology, Nanjing Medical University, Nanjing, Jiangsu, China

ABSTRACT

Core binding factor beta (*Cbfb*) is essential for embryonic bone morphogenesis. Yet the mechanisms by which *Cbfb* regulates chondrocyte proliferation and differentiation as well as postnatal cartilage and bone formation remain unclear. Hence, using *paired-related homeobox transcription factor 1*-Cre (*Prx1*-Cre) mice, mesenchymal stem cell-specific *Cbfb*-deficient (*Cbfb*^{fl/fl}*Prx1*-Cre) mice were generated to study the role of *Cbfb* in postnatal cartilage and bone development. These mutant mice survived to adulthood but exhibited severe sternum and limb malformations. Sternum ossification was largely delayed in the *Cbfb*^{fl/fl}*Prx1*-Cre mice and the xiphoid process was noncalcified and enlarged. In newborn and 7-day-old *Cbfb*^{fl/fl}*Prx1*-Cre mice, the resting zone was dramatically elongated, the proliferation zone and hypertrophic zone of the growth plates were drastically shortened and disorganized, and trabecular bone formation was reduced. Moreover, in 1-month-old *Cbfb*^{fl/fl}*Prx1*-Cre mice, the growth plates were severely deformed and trabecular bone was almost absent. In addition, *Cbfb* deficiency impaired intramembranous bone formation both in vivo and in vitro. Interestingly, although the expression of Indian hedgehog (*Ihh*) was largely reduced, the expression of parathyroid hormone-related protein (PTHrP) receptor (PPR) was dramatically increased in the *Cbfb*^{fl/fl}*Prx1*-Cre growth plate, indicating that *Cbfb* deficiency disrupted the *Ihh*-PTHrP negative regulatory loop. Chromatin immunoprecipitation (ChIP) analysis and promoter luciferase assay demonstrated that the *Runx/Cbfb* complex binds putative *Runx*-binding sites of the *Ihh* promoter regions, and also the *Runx/Cbfb* complex directly upregulates *Ihh* expression at the transcriptional level. Consistently, the expressions of *Ihh* target genes, including *CyclinD1*, *Ptc*, and *Pthlh*, were downregulated in *Cbfb*-deficient chondrocytes. Taken together, our study reveals not only that *Cbfb* is essential for chondrocyte proliferation and differentiation for the growth and maintenance of the skeleton in postnatal mice, but also that it functions in upregulating *Ihh* expression to promote chondrocyte proliferation and osteoblast differentiation, and inhibiting PPR expression to enhance chondrocyte differentiation. © 2014 American Society for Bone and Mineral Research.

KEY WORDS: GENETIC ANIMAL MODELS; SIGNALING PATHWAYS; DEVELOPMENT; OSTEOBLASTS; GROWTH PLATE; INDIAN HEDGEHOG

Introduction

Core binding factors (CBFs) are heterodimeric transcription factors composed of two subunits: the core binding factor

alpha (CBF α) and core binding factor beta (CBF β).⁽¹⁾ CBF α subunits are encoded by three genes, namely *Runx-related transcription factor 1* (*Runx1*) (*Cbfa2*), *Runx2* (*Cbfa1*), and *Runx3* (*Cbfa3*),⁽²⁾ each of which plays important roles in skeletal

Received in original form February 25, 2013; revised form December 24, 2013; accepted January 9, 2014. Accepted manuscript online May 12, 2014.

Address correspondence to: Wei Chen, MD, Department of Pathology, University of Alabama at Birmingham, SHEL 810, 1825 University Blvd, Birmingham, AL 5294, USA. E-mail: wechen@uab.edu

Additional Supporting Information may be found in the online version of this article.

*FT and MW contributed equally to this work.

#WC and YPL contributed equally to this work.

Journal of Bone and Mineral Research, Vol. 29, No. 7, July 2014, pp 1564–1574

DOI: 10.1002/jbmr.2275

© 2014 American Society for Bone and Mineral Research

development. Runx2 is a key transcription factor associated with osteoblast differentiation and chondrocyte hypertrophy.⁽³⁾ Runx3 is indispensable for endochondral ossification if the *Runx2* gene dosage is reduced,⁽⁴⁾ and Runx1 cooperates with Runx2 to regulate sternal morphogenesis.^(5,6)

The non-DNA-binding subunit, Cbfb, cooperates with Cbfa to form DNA-protein complexes and protects the Cbfa subunits from degradation.⁽⁷⁾ *Cbfb*^{-/-} embryos died from an absence of fetal liver hematopoiesis at mid-gestation.^(8,9) This barrier had impeded further research in understanding the role of Cbfb in skeletal development until the generation of the three mice models (*Cbfb*^{GFP/GFP} knock-in mice, and *Tek-GFP/Cbfb* and *Gata1-Cbfb* transgenic mice) in 2002.⁽¹⁰⁻¹²⁾ *Cbfb*^{GFP/GFP} knock-in mice died soon after birth. *Cbfb*^{-/-} embryos that were rescued by *Tek-GFP/Cbfb* (*Cbfb*^{-/-}Tg[*Tek-GFP/Cbfb*]) and *Gata1-Cbfb* (*Cbfb*^{-/-}Tg[*Gata1-Cbfb*]) transgene died around birth. These mouse models enabled the study of Cbfb's role in embryonic skeletal development.⁽¹⁰⁻¹²⁾ The role of Cbfb in postnatal bone formation was unexplored until the generation of *Cbfb/Runx2* double transgenic mice, which exhibited severe osteopenia.⁽¹³⁾ However, the physiological defects caused by Cbfb deficiency in postnatal mice have not yet been clarified. To further explore the role of Cbfb in skeletal development, we generated mesenchymal stem cell (MSC)-specific *Cbfb* conditional knockout mice by crossing *Cbfb*^{fl/fl} mice⁽¹⁴⁾ with (*paired-related homeobox transcription factor 1*) *Prx1*-Cre mice.⁽¹⁵⁾ Cre expression driven by the *Prx1*-promoter was first detected in the forelimb mesenchyme at embryonic day (E) 9.5 and then in all MSCs at E10.5.⁽¹⁵⁾ *Cbfb*^{fl/fl} *Prx1*-Cre mice survived into adulthood, *Cbfb*^{fl/fl} *Prx1*-Cre mice displayed short limbs, short statures, inhibited osteoblastogenesis, inhibited chondrocyte differentiation, and impaired trabeculae formation. In addition, Cyclin D1, Indian hedgehog (Ihh), and parathyroid hormone-related protein receptor (PPR) expression were dysregulated in the growth plates of the *Cbfb*^{fl/fl} *Prx1*-Cre mice.

Materials and Methods

Generation of Cbfb conditional knockout mice

Cbfb^{fl/fl} mice (B6.129P2-*Cbfb*^{tm1Itan/J}) mice⁽¹⁴⁾ and *Prx1*-Cre (B6.Cg-Tg[*Prx1*-Cre]1Cjt/J)⁽¹⁵⁾ (Jackson Laboratory, Bar Harbor, MI, USA) were crossed to generate *Cbfb*^{fl/+} *Prx1*-cre mice, and their progeny were intercrossed to obtain *Cbfb*^{fl/fl} *Prx1*-cre mice. Mice were housed in the animal room of University of Alabama at Birmingham (UAB) (Birmingham, AL, USA). All research procedures using mice were approved by the UAB Animal Care and Use Committee and conformed to NIH guidelines.

Statistical analysis and data quantification analysis

All data were presented as the mean \pm SD. Statistical significance was assessed using Student's *t* test performed with the SPSS 16.0 software (SPSS Incorporation, Chicago, IL, USA). Values of $p < 0.05$ were considered significant, and labeled * $p < 0.05$, ** $p < 0.01$, *** $p < 0.001$ in the graphs. The results are representative of at least six individual experiments ($n = 6$).

Results

Spatial and temporal expression of Cbfb in wild-type mouse skeleton

Expression of Cbfb in skeletons at postnatal 1-day-old (P1) mice was detected by immunohistochemistry (IHC) using paraffin

sections. The results showed that Cbfb is highly expressed in proliferative chondrocytes, hypertrophic chondrocytes, and osteoblasts in long bones (Supporting Fig. S1A), vertebrae (Supporting Fig. S1B), and ribs (Supporting Fig. S1C).

MSC-specific Cbfb-deficient mice exhibited dwarfism with skeletal malformation and delayed ossification

MSC-specific *Cbfb*-deficient mice were generated by crossing *Cbfb*^{fl/fl} mice with *Prx1*-cre mice, and genotypes were confirmed by PCR analysis (Fig. 1L). Efficient ablation of Cbfb expression in chondrocytes and osteoblasts in ribs, vertebrae, and long bones in *Cbfb*^{fl/fl} *Prx1*-Cre mice was confirmed by IHC (Supporting Fig. S2A-C). Although a small portion (~10%) of homozygotes died of asphyxiation problems soon after birth, most survived into adulthood. Male homozygotes were fertile. Female homozygotes were able to conceive, although dystocia would occur, probably due to an abnormal pelvis (Fig. 2A, upper panel and lower panel). Postnatal 7-day-old (P7) *Cbfb*^{fl/fl} *Prx1*-Cre mice exhibited dwarfism (Fig. 1A, B) with shortened limbs (Fig. 1A-D) compared to wild-type (WT) cohorts. Bone morphology of P7 mice was analyzed by Alizarin red S/Alcian blue staining (Fig. 1B-I). Although limbs were shortened, the epiphyseal cartilage (light grey color) was elongated (Fig. 1C, D) in the *Cbfb*^{fl/fl} *Prx1*-Cre mice. In addition, mutant mice had widened sutures and enlarged fontanelles, with delayed ossification of the parietal and frontal bones (Fig. 1F). Ossification of the sternum (Fig. 1H) and hyoid bone (Fig. 1I) were also delayed in mutant mice compared to WT mice. The xiphoid process was non-calcified and abnormally enlarged (Fig. 1H). Spines and ribs did not show notable morphological changes in P7 mutant mice (Fig. 1E, G), but they did show delayed ossification in P1 mutant mice (Supporting Fig. S2D, E). Thus, defects may be compensated for as the mice aged. Finally, the short-limb deformity observed in the mutant mice (Fig. 1A-D) persists with age, which was confirmed again by Alizarin red S/Alcian blue (Fig. 1J) and μ CT analysis (Fig. 1K) of 1-month-old (P30) mice. Notably, X-ray analysis showed that 6-week-old *Cbfb*^{fl/fl} *Prx1*-Cre mice displayed several characteristics of cleidocranial dysplasia (eg, short stature, short limb, and absent clavicles) (Fig. 2A). Taken together, these results indicate that loss of Cbfb results in dwarfism, limb and sternum malformation, and delayed skeletal ossification during postnatal skeletal development.

Loss of Cbfb impaired skeletal development in newborn mice

Next, to examine the role of Cbfb in the differentiation of chondrocytes, osteoblasts, and osteoclasts in newborn mice, hematoxylin and eosin (H&E) staining, Safranin O staining, Goldner's trichrome staining, and TRAP staining were performed on paraffin sections of femurs (Fig. 2B-F). Compared with WT mice, newborn *Cbfb*^{fl/fl} *Prx1*-Cre mice had elongated growth plates and shortened diaphysis (Fig. 2B, C). Although the resting zone was elongated, the proliferation zone was shortened and the proliferative columns, which were presented in the WT growth plates, were disrupted in newborn mutant mice (Fig. 2C). The hypertrophic zone was also slightly deformed in newborn mutant mice (Fig. 2C). Furthermore, the number and thickness of trabecular bones and the number of osteoblasts were significantly reduced in newborn *Cbfb*^{fl/fl} *Prx1*-Cre mice (Fig. 2D, E), the osteoclast number did not change (Fig. 2D-F). These results indicate that Cbfb is important for chondrocyte proliferation and

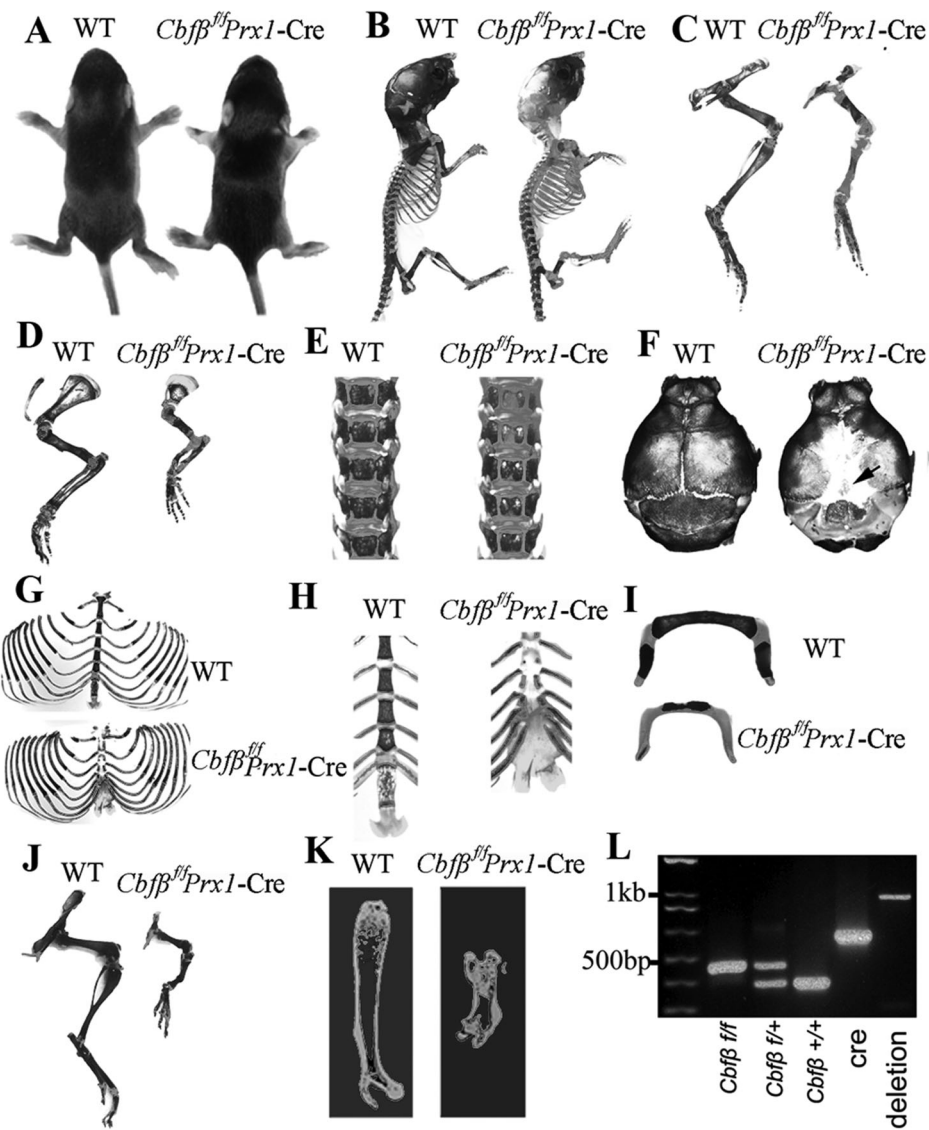


Fig. 1. *Cbfb^{ff}Prx1-Cre* mice had dwarfism with shortened limbs. (A) Gross morphology of postnatal 7-day-old (P7) *Cbfb^{ff}Prx1-Cre* and wild-type (WT) mice. (B–I) Skeletal analysis by Alizarin red S/Alcian blue staining of P7 *Cbfb^{ff}Prx1-Cre* and WT mice. Long bones were shorter (C, D), sutures and fontanelles were widened (black arrow) (F), and ossification of parietal bones (F), frontal bone (F), sternum (H), and hyoid bone (I) was delayed in *Cbfb^{ff}Prx1-Cre* mice. Development of ribs (G) and spine (E) was not affected in *Cbfb^{ff}Prx1-Cre* mice. (J) Skeletal analysis by Alizarin red S/Alcian blue staining of P30 *Cbfb^{ff}Prx1-Cre* and WT mouse limb. (K) μ CT analysis of P30 *Cbfb^{ff}Prx1-Cre* and WT mouse femur. (L) PCR was used to determine *Cbfb* alleles (*f/f*, *f/+*, *+/+*, or deletion) and the presence of Cre.

maturation in newborn mice and that it may play a lesser role in osteoclasts.

Loss of *Cbfb* impaired growth plate development in P7 mice

Continuous postnatal skeletal development is required for normal development toward adulthood. H&E staining on paraffin sections of P7 mouse femur showed that growth plate and trabecular bone development were delayed in mutant mice (Fig. 3A, B). Comparable with the newborn mutant mice (Fig. 2B, C), P7 mutant mice also had shortened femurs, elongated growth plates, shortened diaphysis (Fig. 3A), elongated resting zones,

and shortened and disorganized proliferation zones (Fig. 3B). Although the hypertrophic zone was slightly deformed in newborn mutant mice (Fig. 2C), it was notably shortened in the P7 *Cbfb^{ff}Prx1-Cre* mice (Fig. 3B). Moreover, proliferating cell nuclear antigen (PCNA) staining showed that the number of proliferating chondrocytes was decreased (Fig. 3C, D), and immunofluorescent (IF) staining showed that collagen type X (ColX) expression was reduced in mutant mice compared to WT (Fig. 3E). These results confirmed the retardation of chondrocyte proliferation and hypertrophy in *Cbfb^{ff}Prx1-Cre* mice. Micromass culture of growth plate chondrocytes from newborn mice and Alcian blue staining confirmed that chondrocyte differentiation in vitro was also drastically delayed in the absence of *Cbfb*

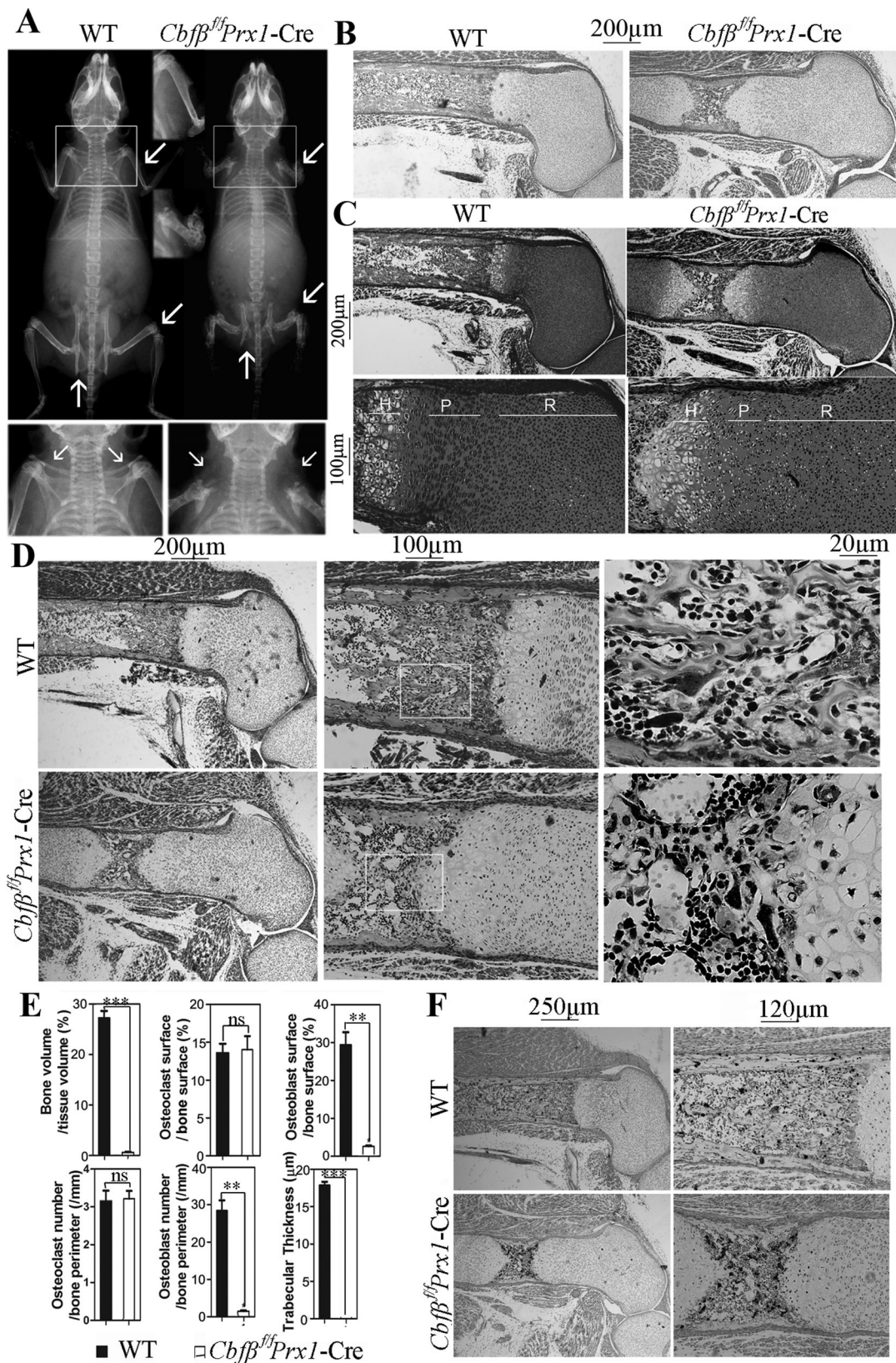


Fig. 2. *Cbfb* deficiency resulted in cleidocranial dysplasia-like phenotype in adult mice and skeletal defects in newborn mice. (A) Whole-body X-ray of 6-week-old mice showed cleidocranial dysplasia-like phenotype of *Cbfb^{fl/fl}Prx1-Cre* mice, including shortened stature, shortened long bones (upper lane, marked by arrowhead), and absent clavicles (lower lane marked by arrowhead and upper lane marked by arrowhead and square). (B) H&E staining of paraffin sections of femurs from newborn *Cbfb^{fl/fl}Prx1-Cre* mice and WT mice. (C) Safranin O staining of paraffin sections of femurs from newborn *Cbfb^{fl/fl}Prx1-Cre* mice and WT mice. (D) Goldner's trichrome staining of paraffin sections of femurs from newborn *Cbfb^{fl/fl}Prx1-Cre* mice and WT mice. (E) Quantification data of Goldner's trichrome staining were presented as mean \pm SD, $n \geq 6$, ns = nonsignificant, ** $p < 0.01$, *** $p < 0.001$ versus WT. (F) TRAP staining of paraffin sections of femurs from newborn *Cbfb^{fl/fl}Prx1-Cre* mice and WT mice. P = proliferation zone; R = resting zone; H = hypertrophic zone.

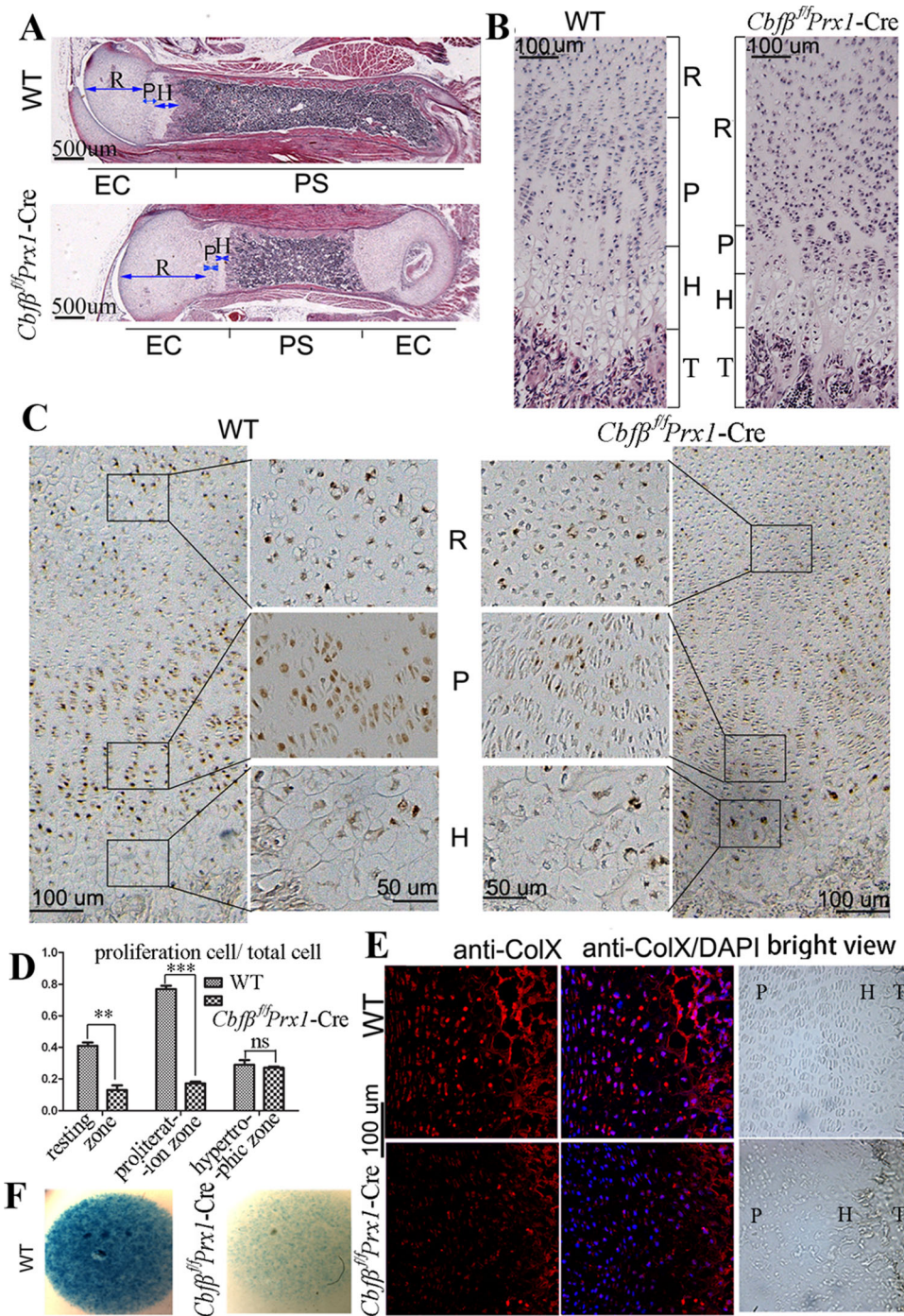


Fig. 3. *Cbfb* deficiency retards the development of primary spongiosa and delays chondrocyte proliferation and maturation. (A, B) H&E staining of paraffin sections of femurs from P7 *Cbfb^{fl/fl}Prx1-Cre* mice and WT mice. Femur and primary spongiosa were shortened, while the epiphyseal growth plate was elongated in *Cbfb^{fl/fl}Prx1-Cre* mice. Columnar structure of proliferative chondrocyte zone was lost in *Cbfb^{fl/fl}Prx1-Cre* mice. (C) PCNA staining of paraffin sections of femurs from P7 *Cbfb^{fl/fl}Prx1-Cre* mice and WT mice. Second and third columns show magnified images of areas in black boxes. (D) The ratio of proliferating cells in total cells in the three chondrocyte zones of WT and *Cbfb^{fl/fl}Prx1-Cre* mice from (C). Data were presented as mean ± SD, $n \geq 6$, ns = nonsignificant, ** $p < 0.01$, *** $p < 0.001$ versus the same zone in WT mice. (E) IF staining using frozen sections of P7 mouse femurs showed that ColX expression was decreased in *Cbfb^{fl/fl}Prx1-Cre* mice. Bright field views were co-presented on the right panel. (F) Micromass culture of growth plate chondrocytes of newborn mice. PS = primary spongiosa; EC = epiphyseal cartilage; R = resting zone; P = proliferation zone; H = hypertrophic zone; T = trabecular bone.

(Fig. 3F). Taken together, these results demonstrate that *Cbfb* plays important roles in growth plate formation in the early stages of postnatal development.

Loss of *Cbfb* blocked *Ihh*-cyclin D1 signaling and the *Ihh*-PTHrP negative feedback loop

Protein expression in the growth plates was detected by IF staining using P7 mouse femur sections (Fig. 4A–D, bright field views are co-presented in Supporting Fig. S3A–D) and Western blot using proteins from newborn mouse femoral cartilage (Fig. 4E, F). Expression of SRY-related high-mobility group-Box gene 9 (*Sox9*), a key transcription factor in the chondrocyte lineage, was similar in WT and *Cbfb^{fl/fl}Prx1-Cre* mice (Figs. 4A; Supporting Fig. S3A). However, expression of *Ihh* was dramatically reduced in *Cbfb^{fl/fl}Prx1-Cre* mice (Fig. 4B, E, F; Supporting Fig. S3B). Cyclin D1, a cell-cycle-regulating protein downstream of *Ihh*,⁽¹⁶⁾ was also decreased in the proliferation zone of *Cbfb^{fl/fl}Prx1-Cre* femurs (Fig. 4C, E, F; Supporting Fig. S3C), which may inhibit chondrocyte proliferation. Consistently, expression of other *Ihh*-targeted genes besides Cyclin D1 (eg, *Pthlh* and *Patched* [*PTC*]) were also reduced in the growth plates of *Cbfb^{fl/fl}Prx1-Cre* mice. qRT-PCR using mRNA from newborn mouse femur showed that *Pthlh* expression was reduced by 30% in *Cbfb^{fl/fl}Prx1-Cre* mice (Supporting Fig. S5B). IHC staining using P7 mouse femur sections showed that *PTC* expression was detected in the prehypertrophic zone in the growth plates in WT mice, but that it was greatly reduced in mutant mice (Fig. 4G). *Ihh* induces PTHrP expression in periarticular cells around prehypertrophic chondrocytes, which in turn suppresses chondrocyte differentiation through a feedback regulatory process, the “*Ihh*-PTHrP negative feedback loop.”⁽¹⁷⁾ Interestingly, although *Ihh* and *Pthlh* expression were reduced, PPR expression was increased in the *Cbfb^{fl/fl}Prx1-Cre* growth plate. Upregulation of PPR in *Cbfb^{fl/fl}Prx1-Cre* mice may increase the sensitivity of chondrocytes to PTHrP and retard chondrocyte hypertrophy even in the presence of a permissive dose of PTHrP resulting from decreased *Ihh* expression. In conclusion, *Cbfb* deficiency may affect chondrocyte proliferation by inhibiting *Ihh*-cyclin D1 signaling and interfere with normal chondrocyte hypertrophy by disturbing the *Ihh*-PTHrP negative feedback loop.

Runx/Cbfb complex regulated *Ihh* expression by binding to the *Ihh* promoter directly

In order to determine if the *Runx/Cbfb* complex binds the promoter region of *Ihh*, chromatin immunoprecipitation (ChIP) assay was performed using anti-*Cbfb* antibody and the primers shown in Fig. 4H. The ChIP input value using each primer pair represents the binding efficiency of its adjacent region. There were 16 predicted *Runx*-binding sites localizing in the *Ihh* promoter region (–3919/+27) (Fig. 4H). Primer pairs 4 and 5 resulted in the highest values (Fig. 4I), indicating that *Runx2/Cbfb* complex may bind sites 9 through 16 most efficiently. A 1.4-kb *Ihh* promoter region (–1287/+162), which contains *Runx*-binding sites 9 through 16, was cloned into the pGL3-basic vector. Luciferase activity driven by the *Ihh* promoter (–1287/+162) was low in the *Cbfb^{fl/fl}Prx1-Cre* chondrocytes and robustly increased (10-fold) after the expression of *Cbfb* (Fig. 4J). Ectopic expression of *Runx2* further promoted the luciferase signal. In conclusion, we believe that the *Runx/Cbfb* heterodimer directly binds to the *Runx*-binding sites of the *Ihh* promoter regions and upregulates *Ihh* expression at the transcriptional level.

Trabecular bone formation is impaired in MSC-specific *Cbfb*-deficient mice

Delayed ossification was observed in P1 (Supporting Fig. S2D, E), P7 (Fig. 1), and 6-week-old (Fig. 2A) *Cbfb^{fl/fl}Prx1-Cre* mice. This was further confirmed by the H&E staining of P30 mice paraffin sections, which revealed a dramatic loss of trabecular bone in mutant mice (Fig. 5A, B). Notably, the growth plates were also severely deformed, protruding deep into the diaphysis (Fig. 5B, arrow). To investigate the potential role of *Cbfb* in osteoblasts in vivo, IF staining using mouse femur sections was performed (Fig. 5C–F; Supporting Fig. S4). Expression of *Runx2* (a master transcription factor in the osteoblast lineage) was similar in P7 WT and *Cbfb^{fl/fl}Prx1-Cre* growth plates and trabecular bone, and increased in mutant perichondrium (Fig. 5E). Expression of *Runx3*, detected mainly in hypertrophic and prehypertrophic chondrocytes, was also similar between E18.5 and E16.5 WT and mutant femur (Supporting Fig. S4). However, *Osx* (*Osterix*) (Fig. 5C) and *Opn* (*Osteopontin*) (Fig. 5D), which are osteoblast-related genes, showed reduced expression in P7 *Cbfb^{fl/fl}Prx1-Cre* trabecular bone compared with WT, indicating that osteoblastogenesis may be influenced. In addition, vascular endothelial growth factor (VEGF) expression was downregulated in the growth plates of newborn mutant mice (Fig. 5F). Decreased VEGF expression results in reduced angiogenesis, which may affect the population of MSC for normal trabecular bone formation. Taken together, these data demonstrate that *Cbfb* not only regulates chondrocyte proliferation and maturation, but also influences trabecular bone formation for normal skeleton morphogenesis.

Loss of *Cbfb* impaired osteoblastogenesis of calvarial cells in vitro

To further confirm the role of *Cbfb* in bone ossification, we investigated the role of *Cbfb* in osteoblastogenesis in vitro using osteoblast derived from calvarial cell primary culture (Fig. 6). Deletion of *Cbfb* expression in *Cbfb^{fl/fl}Prx1-Cre* osteoblasts was confirmed by quantitative RT-PCR (qRT-PCR) (Fig. 6C) and Western blot (Fig. 6G). *Cbfb^{fl/fl}Prx1-Cre* osteoblasts showed reduced alkaline phosphatase (ALP) activity (Fig. 6A) and mineralization (Fig. 6B) compared to WT cells, indicating that osteoblastogenesis was impeded in mutant cells. qRT-PCR revealed that the osteoclastogenesis related cytokines *receptor activator of nuclear factor- κ B ligand* (*RANKL*) was similarly expressed in *Cbfb^{fl/fl}Prx1-Cre* and WT osteoblasts (Fig. 6F). Expression of the osteoblast-related gene *Ocn* (*Osteocalcin*) was decreased in *Cbfb^{fl/fl}Prx1-Cre* cells on day 7 of osteoblastogenesis (Fig. 6D), and the expression of *Ocn*, *Opn*, *Alp*, and *integrin binding sialoprotein* (*Ibsp*) was also decreased in *Cbfb^{fl/fl}Prx1-Cre* cells on day 14 of osteoblastogenesis (Fig. 6E, F). However, *Runx2* expression was increased (Fig. 6D, E), especially isoform 1 of *Runx2* (*Runx2-l*) (Fig. 6H). The expression of *Osx*, another master transcription factor of osteoblast differentiation, was also similar in WT and *Cbfb*-deficient cells (Fig. 6D, E). Considering that *Osx* expression was decreased in *Cbfb^{fl/fl}Prx1-Cre* trabecular bone (Fig. 5C), the mechanism by which *Runx2* regulates *Osx* expression may be different in calvaria and long bones. Western blot revealed that protein levels of *Runx2* and *Runx3* were not affected, but that expression of *Ocn* and *Runx1* was reduced in *Cbfb^{fl/fl}Prx1-Cre* osteoblasts on day 14 and 21 of osteoblastogenesis. When *Runx1* expression was selectively rescued in the endothelial and hematopoietic systems of *Runx1^{-/-}* embryos (*Runx1^{Re/Re}* mice), these mice survived until birth and displayed

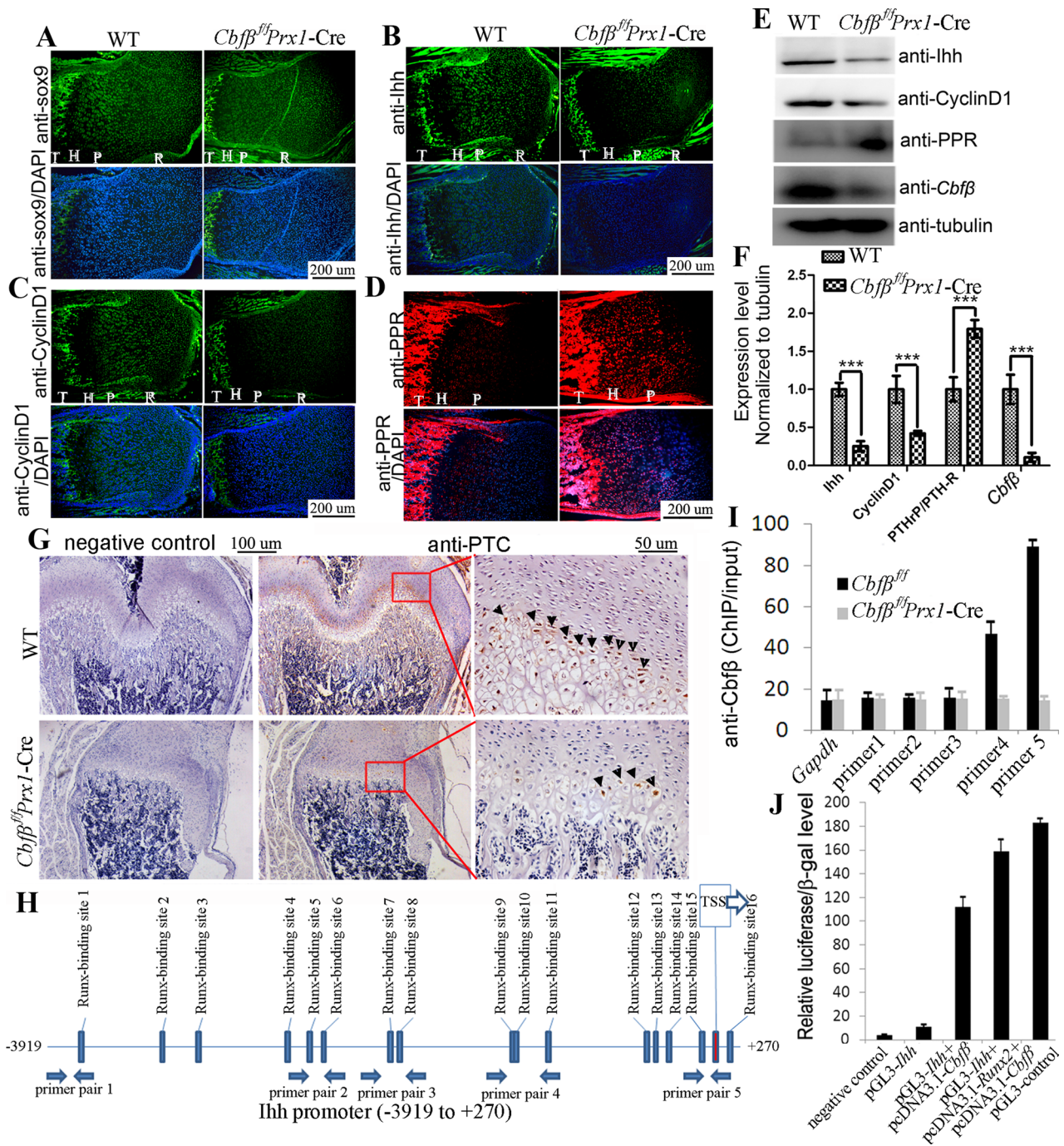


Fig. 4. Expression of Sox9, Ihh, CyclinD1, PTHrP-R, and Cbfb in chondrocytes of *Cbfb^{fl/fl}Prx1-Cre* mice and WT mice. Similar Sox9 expression (A), decreased Ihh expression (B), decreased Cyclin D1 expression (C), and increased PPR expression (D) was observed in femur growth plates of P7 *Cbfb^{fl/fl}Prx1-Cre* mice compared to that of WT mice, as detected by IF staining using frozen sections. (E) The expression of Ihh, CyclinD1, PPR, and Cbfb was confirmed by Western blot using protein lysates of femoral cartilage from *Cbfb^{fl/fl}Prx1-Cre* and WT newborn mice. (F) Protein levels in E were quantified and normalized to tubulin. (G) The expression of Patched (PTC) in the prehypertrophic zone of the growth plates in P7 *Cbfb^{fl/fl}Prx1-Cre* mice was reduced compared with that in WT mice, as detected by IHC staining using paraffin sections. Third column shows the magnified images of areas in red boxes. Arrowheads indicate positive stains. (H) Schematic display of the *Ihh* promoter region (-3919/+270). TSS (transcriptional start site), predicted Runx-binding sites and ChIP primer positions were indicated in the figure. (I) ChIP was performed using WT chondrocyte lysates, anti-Cbfb antibody, and primers as indicated in H. (J) The *Ihh* promoter region (-1287/+162) was inserted into the pGL3-basic vector. Primary *Cbfb^{fl/fl}Prx1-Cre* chondrocytes were transfected with pGL3-control, pGL3-*Ihh* + pcDNA3.1a-Cbfb, or pGL3-*Ihh* + pcDNA3.1a-Cbfb + pcDNA3.1a-*Runx2*. The β-GAL-expression plasmid was also cotransfected. Luciferase activity was detected 48 hours posttransfection, and normalized to β-GAL activity. Data were presented as mean ± SD, $n \geq 6$, ns = nonsignificant, *** $p < 0.001$. R = resting zone; P = proliferation zone; H = hypertrophic zone; T = trabecular bone.

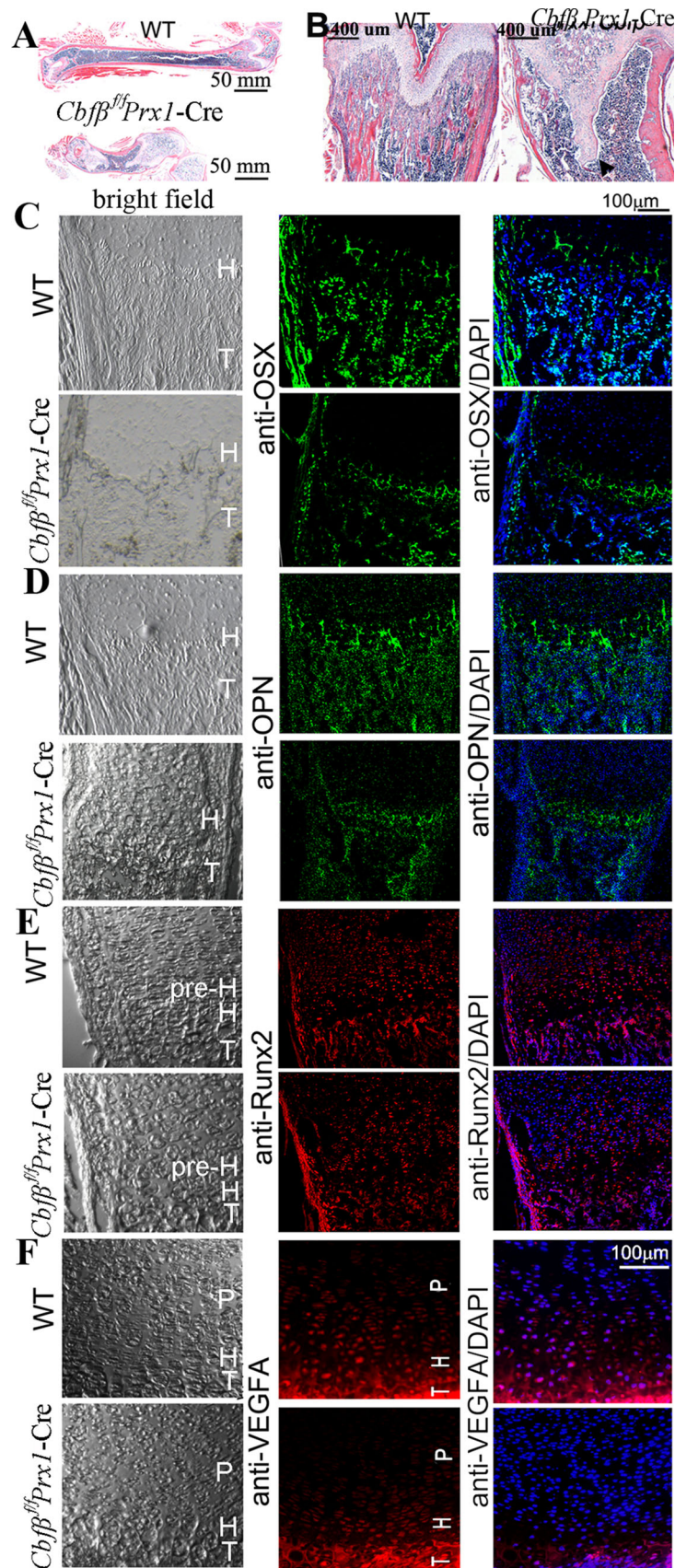


Fig. 5. Mice lacking *Cbfb* had delayed ossification. (A, B) H&E staining of the femurs of P30 (postnatal 1-month-old) WT and *Cbfb^{fl/fl}Prx1-Cre* mice. The femur was shortened and trabecular bone was lost in *Cbfb^{fl/fl}Prx1-Cre* mice. The epiphyseal growth plate protruded deep into the diaphysis abnormally (marked by arrowhead). (C–F) IF staining using frozen sections of femurs of P7 (C–E) and newborn (F) WT and *Cbfb^{fl/fl}Prx1-Cre* mice. In the *Cbfb^{fl/fl}Prx1-Cre* mice, expression of OSX (C), OPN (D), and VEGFA (F) was decreased, but expression of Runx2 (E) was not changed. Bright field views of C–F are co-presented on the left panel. T = trabecular bone; H = hypertrophic zone; P = proliferation zone; pre-H = prehypertrophic zone.

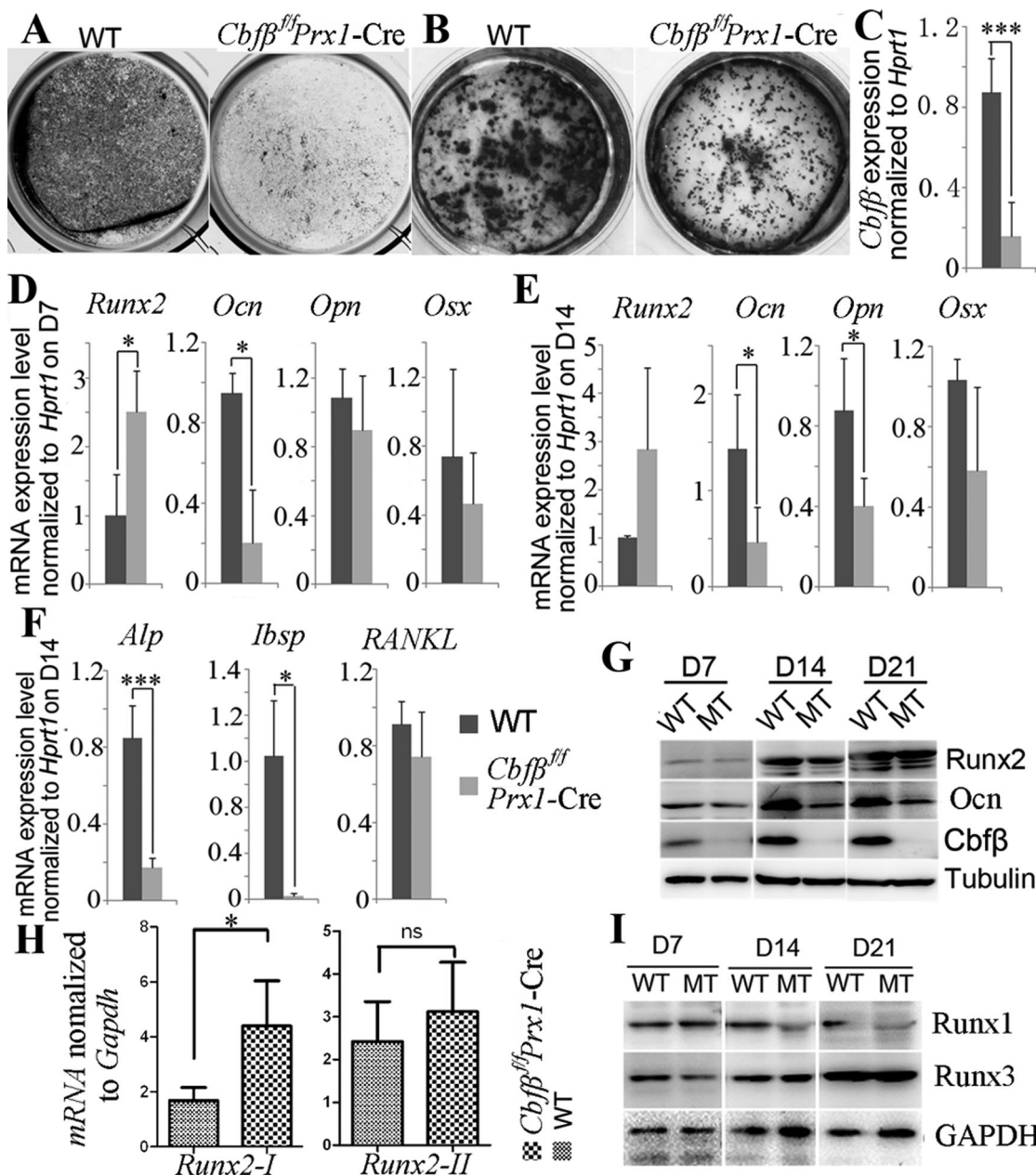


Fig. 6. *Cbfb* is required for osteoblastogenesis of calvarial cells. Calvarial cells from *Cbfb^{ff/Prx1-Cre}* and WT newborn mice were used for primary culture. Osteoblastogenesis was detected by (A) ALP staining on day 14 of osteoblastogenesis and mineralization was detected by (B) Von Kossa staining on day 21 of osteoblastogenesis. (C) *Cbfb* expression levels in calvarial cells were detected by qRT-PCR and normalized to *Hprt1*. (D, E) Expression of *Runx2*, *Opn*, *Ocn*, and *Osx* in calvarial cells on day 7 (D7) (D) and day 14 (D14) (E) of osteoblastogenesis was detected by qRT-PCR and normalized to *Hprt1*. (F) Expression of *Alp*, *Ibsp*, and *RANKL* in calvarial cells on day 14 of osteoblastogenesis was detected qRT-PCR and normalized to *Hprt1*. (G) Western blot was applied to detect the protein levels of *Runx2*, *Ocn*, and *Cbfb* in WT and mutant (MT) calvarial cells on days 7, 14, and 21 (D7, D14, and D21, respectively) of osteoblastogenesis. (H) Expression levels of *Runx2-I* and *Runx2-II* in calvaria were determined by qRT-PCR and normalized to *Gapdh*. (I) Western blot was applied to detect the protein levels of *Runx1* and *Runx3* in WT and mutant calvarial cells on days 7, 14, and 21 of osteoblastogenesis. Results were presented as mean \pm SD, $n \geq 6$, ns = nonsignificant, * $p < 0.05$, *** $p < 0.005$.

disrupted mineralization in some skull elements,⁽⁶⁾ indicating that *Runx1* plays a role in calvarial osteoblastogenesis. Thus, *Runx1* hyposufficiency in *Cbfb^{ff/Prx1-Cre}* cells may partially contribute to the impeded osteoblast differentiation. Taken together, these results indicate that *Cbfb* deficiency affects osteoblast differentiation in vitro.

Discussion

The *Ihh*-PTHrP negative feedback loop maintains chondrocyte proliferation and counters chondrocyte hypertrophy.⁽¹⁷⁾ We report that *Cbfb* plays a dual function in this loop by regulating the expression of *Ihh* and PPR (Fig. 4B, D), thereby affecting the

balance of chondrocyte proliferation and maturation. The Runx/Cbfb complex binds the promoter region of the *Ihh* gene so as to regulate its expression (Fig. 4H–J). Consistently, diminished *Ihh* expression was also observed in *Runx2*^{-/-} and *Runx2*^{-/-}*Runx3*^{-/-} mice.⁽⁴⁾ It is therefore possible that Cbfb also regulates the *Ihh*-PTHrP negative feedback loop by interacting with Runx2 and Runx3, thereby regulating chondrocyte proliferation and maturation. Thus, Cbfb deficiency results in impaired growth plates development (Figs. 2 and 3) and severe skeletal malformation (Fig. 1).

Runx2 is a master regulator of the commitment and differentiation of pluripotent MSCs to osteoblasts.⁽³⁾ As a subunit of the CBF complex, Cbfb interacts with Runx2 to stabilize its interaction with DNA. pGL3-3XOSE2 was constructed by inserting three *OSE2*,⁽¹⁸⁾ a Runx2 binding sequence, into the pGL3-promoter. If only Runx2 and Cbfb were co-expressed, luciferase driven by the promoter with the *OSE2* sequence increased 1.7-fold (Supporting Fig. S5A), indicating that Runx activities were deregulated in the *Cbfb*-deficient cells. Thus, *Cbfb*^{fl/Prx1}-Cre mice at birth displayed a similar, but less severe, phenotype to *Runx2*^{-/-} mice⁽³⁾ (eg, reduced ossification and inhibited chondrocyte hypertrophy). Consistently, expression of Runx2 targeted genes, *ColX* (Fig. 3E) and *Ocn* (Fig. 6D, E), were also downregulated in *Cbfb*-deficient mice. Although *Cbfb* has been reported to protect the Cbfa subunits from degradation,⁽⁷⁾ only Runx1 expression was reduced in *Cbfb*^{fl/Prx1}-Cre calvarial cells compared to WT (Fig. 6I), and Runx2 and Runx3 were similarly expressed in WT and *Cbfb*^{fl/Prx1}-Cre calvarial cells and long bones (Figs. 6G, I, 5E; Supporting Fig. S4). In fact, Runx2 expression was higher in *Cbfb*^{fl/Prx1}-Cre perichondrium compared to WT (Fig. 5E). Expression of *Runx2-I*, a specific *Runx2* isoform expressed in the perichondrium and proliferating chondrocytes,⁽¹⁹⁾ was also increased in *Cbfb*^{fl/Prx1}-Cre calvaria (Fig. 6H). Thus, the protection mechanism of Runx proteins may vary depending on the cell type and the differentiation stage. In addition, the high expression of Runx2 in the mutant mice, where it would not normally have such high expression, may indicate the immaturity of the cells.

Although the *Runx2*^{-/-} skeletal system showed a complete lack of ossification,⁽³⁾ *Cbfb*-deficient mice only have delayed ossification. The delayed mineralization observed in the ribs and spines in some mice at birth became less severe as the mice aged. This indicates that Runx2 remains partially active without Cbfb. The in vitro promoter assay showed that the two isoforms of *Runx2* (ie, *Runx2-I* and *Runx2-II*) retained some transcriptional activity in the absence of Cbfb.⁽¹³⁾ qRT-PCR showed that *Runx2-I* expression was increased in *Cbfb*-deficient calvaria (Fig. 6H). The partially rescued phenotype of *Cbfb*-deficient mice may be a combined action of the remaining activity of *Runx2-I* and *Runx2-II*.

Cbfb may form a complex with Runx2 or Runx3 to regulate *Ihh* expression, and thereby regulate chondrocyte proliferation and maturation. Recent studies have shown that the Cbfb/Runx1 complex plays an important role in chondrogenesis and chondrocyte proliferation.⁽²⁰⁾ Song and colleagues⁽²¹⁾ reported that Runx1 is required for endochondral ossification during skeletal development. Moreover, Runx1 and Cbfb both have much higher expression levels in MSCs and chondrocytes than Runx2 and Runx3 do.⁽²¹⁾ In addition, Runx2 is usually considered as a positive regulator in chondrocyte maturation rather than in chondrocyte proliferation.^(22,23) All these studies indicate that the Runx1/Cbfb complex may exert a more important role than Runx2/Cbfb and Runx3/Cbfb in chondrocyte proliferation. To our

knowledge, our study is the first report of Cbfb regulating chondrocyte proliferation. Additional studies are needed to characterize the mechanism underlying the roles of Runx/Cbfb complexes in regulating the chondrocyte proliferation in vivo.

In summary, we investigated the role of Cbfb in postnatal cartilage and bone development. We found that Cbfb is a key factor for chondrocyte proliferation, chondrocyte differentiation, and the maintenance of growth plates and trabecular bone in postnatal mice. Cbfb upregulated *Ihh* and downregulated PPR in postnatal growth plates and thereby controlled the proliferation of chondrocytes to prehypertrophic chondrocytes. Our results also indicate that Cbfb may interact with Runx1 to regulate chondrocyte proliferation.

Disclosures

All authors state that they have no conflicts of interest.

Acknowledgments

This work was supported by NIH grants AR-055307 (Y.P.L.) and R01-AR-44741 (Y.P.L.). We thank Mr. Matthew McConnell and Dr. Joel Jules for their extensive reading, discussion, and excellent assistance with this manuscript. We thank Ms. Christie Paulson for her excellent assistance with the manuscript. We thank Mr. Matthew McConnell for his excellent assistance with bioinformatics work and ChIP primer design. We appreciate the assistance of the Center for Metabolic Bone Disease at the University of Alabama at Birmingham (UAB) (P30 AR046031). We are also grateful for the assistance of the Small Animal Phenotyping Core, Metabolism Core, and Neuroscience Molecular Detection Core Laboratory at UAB (P30 NS0474666).

Authors' roles: Study design: YPL and WC. Study conduct: FT, MW, WC, JM, GZ, and BG. Data collection and analysis: MW, FT, WC, LD, JM, GZ, BG, LW, and YPL. Drafting manuscript: MW, WC, FT, and YPL. Revising manuscript: MW, WC, and YPL. All authors approved the final version of the manuscript for submission. WC (wechen@uab.edu) and YPL (ypli@uab.edu) take responsibility for the integrity of data analysis.

References

1. Speck NA, Terry S. A new transcription factor family associated with human leukemias. *Crit Rev Eukaryot Gene Expr*. 1995;5(3–4):337–64.
2. Levanon D, Negreanu V, Bernstein Y, Bar-Am I, Avivi L, Groner Y. AML1, AML2, and AML3, the human members of the runt domain gene-family: cDNA structure, expression, and chromosomal localization. *Genomics*. 1994;23(2):425–32.
3. Komori T, Yagi H, Nomura S, et al. Targeted disruption of *Cbfa1* results in a complete lack of bone formation owing to maturational arrest of osteoblasts. *Cell*. 1997;89(5):755–64.
4. Yoshida CA, Yamamoto H, Fujita T, et al. Runx2 and Runx3 are essential for chondrocyte maturation, and Runx2 regulates limb growth through induction of Indian hedgehog. *Genes Dev*. 2004;18(8):952–63.
5. Kimura A, Inose H, Yano F, et al. Runx1 and Runx2 cooperate during sternal morphogenesis. *Development*. 2010;137(7):1159–67.
6. Liakhovitskaia A, Lana-Elola E, Stamateris E, Rice DP, van 't Hof RJ, Medvinsky A. The essential requirement for Runx1 in the development of the sternum. *Dev Biol*. 2010;340(2):539–46.
7. Huang G, Shigesada K, Ito K, Wee HJ, Yokomizo T, Ito Y. Dimerization with PEBP2beta protects RUNX1/AML1 from ubiquitin-proteasome-mediated degradation. *EMBO J*. 2001;20(4):723–33.
8. Sasaki K, Yagi H, Bronson RT, et al. Absence of fetal liver hematopoiesis in mice deficient in transcriptional coactivator core binding factor beta. *Proc Natl Acad Sci U S A*. 1996;93(22):12359–63.

9. Wang Q, Stacy T, Miller JD, et al. The CBFbeta subunit is essential for CBFalpha2 (AML1) function in vivo. *Cell*. 1996;87(4):697–708.
10. Kundu M, Javed A, Jeon JP, et al. Cbfbeta interacts with Runx2 and has a critical role in bone development. *Nat Genet*. 2002;32(4):639–44.
11. Miller J, Horner A, Stacy T, et al. The core-binding factor beta subunit is required for bone formation and hematopoietic maturation. *Nat Genet*. 2002;32(4):645–9.
12. Yoshida CA, Furuichi T, Fujita T, et al. Core-binding factor beta interacts with Runx2 and is required for skeletal development. *Nat Genet*. 2002;32(4):633–8.
13. Kanatani N, Fujita T, Fukuyama R, et al. Cbf beta regulates Runx2 function isoform-dependently in postnatal bone development. *Dev Biol*. 2006;296(1):48–61.
14. Naoe Y, Setoguchi R, Akiyama K, et al. Repression of interleukin-4 in T helper type 1 cells by Runx/Cbf beta binding to the Il4 silencer. *J Exp Med*. 2007;204(8):1749–55.
15. Logan M, Martin JF, Nagy A, Lobe C, Olson EN, Tabin CJ. Expression of Cre Recombinase in the developing mouse limb bud driven by a Prxl enhancer. *Genesis*. 2002;33(2):77–80.
16. Long F, Zhang XM, Karp S, Yang Y, McMahon AP. Genetic manipulation of hedgehog signaling in the endochondral skeleton reveals a direct role in the regulation of chondrocyte proliferation. *Development*. 2001;128(24):5099–108.
17. Kronenberg HM. Developmental regulation of the growth plate. *Nature*. 2003;423(6937):332–6.
18. Ducy P, Karsenty G. Two distinct osteoblast-specific cis-acting elements control expression of a mouse osteocalcin gene. *Mol Cell Biol*. 1995;15(4):1858–69.
19. Xiao ZS, Hjelmeland AB, Quarles LD. Selective deficiency of the “bone-related” Runx2-II unexpectedly preserves osteoblast-mediated skeletogenesis. *J Biol Chem*. 2004;279(19):20307–13.
20. Johnson K, Zhu S, Tremblay MS, et al. A stem cell-based approach to cartilage repair. *Science*. 2012;336(6082):717–21.
21. Soung do Y, Talebian L, Matheny CJ, et al. Runx1 dose-dependently regulates endochondral ossification during skeletal development and fracture healing. *J Bone Miner Res*. 2012;27(7):1585–97.
22. Enomoto H, Enomoto-Iwamoto M, Iwamoto M, et al. Cbfa1 is a positive regulatory factor in chondrocyte maturation. *J Biol Chem*. 2000;275(12):8695–702.
23. Drissi MH, Li X, Sheu TJ, et al. Runx2/Cbfa1 stimulation by retinoic acid is potentiated by BMP2 signaling through interaction with Smad1 on the collagen X promoter in chondrocytes. *J Cell Biochem*. 2003;90(6):1287–98.